K. Ganesh Kumar, N.G.Rudraswamy*, B.J. Gireesha, and M.R.Krishnamurthy

Influence of nonlinear thermal radiation and viscous dissipation on three-dimensional flow of Jeffrey nano fluid over a stretching sheet in the presence of Joule heating

https://doi.org/10.1515/nleng-2017-0014
Received January 26, 2017; accepted March 11, 2017.

Abstract: Present exploration discusses the combined effect of viscous dissipation and Joule heating on three dimensional flow and heat transfer of a Jeffrey nanofluid in the presence of nonlinear thermal radiation. Here the flow is generated over bidirectional stretching sheet in the presence of applied magnetic field by accounting thermophoresis and Brownian motion of nanoparticles. Suitable similarity transformations are employed to reduce the governing partial differential equations into coupled nonlinear ordinary differential equations. These nonlinear ordinary differential equations are solved numerically by using the Runge–Kutta–Fehlberg fourth–fifth order method with shooting technique. Graphically results are presented and discussed for various parameters. Validation of the current method is proved by comparing our results with the existing results under limiting situations. It can be concluded that combined effect of Joule and viscous heating increases the temperature profile and thermal boundary layer thickness.

Keywords: Three-dimensional flow, Jeffry nanofluid, viscous dissipation, nonlinear thermal radiation, Joule heating, Soret and Dufour

***Corresponding Author: N.G.Rudraswamy:** Department of Studies and Research in Mathematics, Kuvempu University, Shankaraghatta-577 451, Shimoga, Karnataka, India and Department of Mathematics, Sahyadri Science College, Shivamogga-577203, Karnataka, India, E-mail: ngrudraswamy@gmail.com

K. Ganesh Kumar, B.J. Gireesha, M.R.Krishnamurthy: Department of Studies and Research in Mathematics, Kuvempu University, Shankaraghatta-577 451, Shimoga, Karnataka, India, E-mail: ganikganesh@gmail.com, bjgireesu@gmail.com, kittysa.mr@gmail.com

1 Introduction

It is renowned that the non-Newtonian liquids which are quite interesting in contradistinctive applications. The examples of such applications in clued plastics manufacturing, wire and blade coating, dying of paper and textile, polymer industries, food processing, drilling mud, clastomers, certain oils, greases and many others. Thus, the different types of non-Newtonian models are offered in the literature. The present fluid model is known as the Jeffrey fluid. This model is the linear viscoelastic fluid and has an advantage of Maxwell model because of its extra feature about the ratio of relaxation to retardation times. Andersson et al. [1] inspected the MHD flow of an electrically conducting power-law fluid over a stretching sheet in the presence of a uniform transverse magnetic field. Liao [2] approaches the analytic solutions of viscous flows of non-Newtonian fluids over a stretching sheet. The boundary layer flow and heat transfer characteristics of a non-Newtonian viscoelastic fluid over a flat sheet with a linear velocity in the presence of thermal radiation and non-uniform heat source has been carried out by Subhas and Mahesha [3]. The steady two-dimensional stagnation point flow of an incompressible micropolar fluid over a stretching sheet has been analyzed by Nazar et al. [4]. Bhatnagar et al. [5] studied the flow of an Oldroyd-B fluid occupying the space over an elastic sheet, due to the stretching of the sheet, in the presence of a constant free-stream velocity. Cortell [6] considered a numerical study of the flow of an electrically conducting power-law fluid in the presence of a uniform transverse magnetic field.

Radiation heat transfer is also important role in forced and free convection flows, manufacturing of plastic and rubber sheets, glass blowing, metallurgical processes, crystal growing, drawing of continuous filaments through quiescent fluids, gas turbines, annealing and tinning of copper wires, continuous cooling and fiber spinning, design of reliable equipment's, nuclear plants, etc. Keeping all these applications in mind, many authors studied vari-

ous research problems for the case of radiation heat transfer. Bataller [7] initiated the flow and heat transfer of an incompressible second-grade fluid over a non-isothermal stretching sheet in the presence of non-uniform internal heat generation/absorption. The boundary layer flow and heat transfer of viscoelastic fluid flow over stretching sheet in the presence of induced magnetic field and nonlinear thermal radiation have been transmitted by Animasaun et al. [8]. Siddheshwar and Mahabaleshwar [9] investigated the MHD flow and also heat transfer in a viscoelastic liquid over a stretching sheet in the presence of radiation. Aliakbar et al. [10] discussed the flow induced in a viscoelastic fluid by a linearly stretched sheet and assuming that the fluid is Maxwellian and the sheet is subjected to a transverse magnetic field. [11] [12] and [13] are some of the works associated with radiation heat transfer over a stretching sheet problem.

Viscous dissipation affects the heat transfer rate by playing a role like an energy source, which leads to affected rate of heat transfer. The merit of the effect of viscous dissipation depends on whether the plate is being cooled or heated. As the heat-treated materials traveling between a feed roll and wind-up roll or materials manufactured by extrusion, cooling of metallic sheets or electronic chips, glass-fiber and paper production. In view of all these aspects, Chiam [14] analyzed the problem on MHD heat transfer over a non-isothermal stretching sheet, taking into account the suction or blowing at the surface as well as the viscous dissipation and Joule effect. Cortell [15] performed the flow and heat transfer of boundary-layer flow of an electrically conducting fluid of second grade in presence of viscous dissipation. Mohammadein and Gorla [16] presented a boundary layer analysis to study the heat transfer characteristics of a laminar micropolar fluid over a linearly stretching, continuous surface with the effect of viscous dissipation and internal heat generation. The influence of thermal radiation and joule heating effects on MHD flow of an Oldroyd-b fluid with thermophoresis has been investigated by Hayat and Alsaedi [17].

On the other hand, the Soret effect has been also utilized for isotope separation and in a mixture of gasses with very light molecular weight, such as H_2 or He, and of medium molecular weight, such as H_2 or air. In many studies Dufour and Soret effect are neglected, on the basis that they are of a smaller order of magnitude than the effects described by Fourier's and Fick's laws. Kafoussias and Williams [18] analyzed the thermal-diffusion and diffusion-thermo effects on mixed free-forced convective and mass transfer boundary layer flow with temperature dependent viscosity. Srinivasacharya and Kaladhar [19] discussed the mixed convection flow of couple stress fluid in a non-darcy porous medium with Soret and Dufour effects. Hayat et al. [20] initiated the Soret and Dufour effects on the magnetohydrodynamic (MHD) flow of Casson fluid. MHD three-dimensional boundary layer flow of Casson nanofluid past a linearly stretching sheet with convective boundary condition has been carried out by Sohail [21]. Sulochana et al. [22] examined the non-uniform heat source or sink effect on the flow of 3D Casson fluid in the presence of soret and thermal radiation. Anbuchezhian et al. [23] initiated thermophoresis and Brownian motion effects on boundary layer flow of nanofluid in the presence of thermal stratification due to solar energy.

In recent years, the importance of nanofluids have been simulated significantly because of their potential applications in industrial processes such as in chemical processes, heating or cooling processes, power generation and so on. Choi [24] instigated the concept of the nanofluid in the beginning. Nanofluid is a dilute suspension of base fluid and nanoparticles. To upgrade the thermal performance of the base fluid, an innovative technique of adding additives into the base fluid is applied. The problem of laminar fluid flow which results from the stretching of a flat surface in a nanofluid has been inspected by Khan and Pop [25]. Mustafa et al. [26] cross-examined the flow of a nanofluid near a stagnation point towards a stretching surface. Makinde et al. [27] measured the combined effects of buoyancy force, convective heating on stagnation-point flow and heat transfer due to nanofluid flow over a stretching sheet. [28], [29], [30] and [31] are some of them which are focused on nanofluids for both Newtonian and non-Newtonian fluid models.

In all the above-mentioned attempts, the flow is considered to be two-dimensional. Moreover, the flow past a stretching sheet need not be necessarily two-dimensional because the stretching of the sheet can take place in a variety of ways. With the theory proposed by Wang [32] on three-dimensional boundary layer flow induced by a stretching surface, Hayat et al. [33] inspected the MHD three-dimensional flow of nanofluid with velocity slip and nonlinear thermal radiation. Ahmad et al. [34] explored the influence of variable thermal conditions for the heat transfer analysis of a magnetohydrodynamic Maxwell fluid in a porous medium. Khan and Mustafa [35] investigated the MHD three-dimensional flow of upper-convected Maxwell (UCM) fluid over a bi-directional stretching surface by considering the Cattaneo-Christov heat flux model. The magnetohydrodynamic (MHD) three-dimensional flow of Sisko nanofluid bounded by a surface stretched bi-directionally. The nanofluid model includes the Brownian motion and thermophoresis and heat transfer through convective condition have been hypothesized

by Hayat et al. [36]. Ramzan and Bilal [37] determined the magnetohydrodynamic (MHD) three-dimensional flow of an elastico-viscous nanofluid under the influence of mass transfer and chemical reaction. Shehzad et al. [38] postulate the three-dimensional hydromagnetic flow of Jeffrey fluid with nanoparticles and flow is generated by a bidirectional stretching surface. Recent observations on three-dimensional boundary layer flow of Jeffrey nanofluid are noted in Hayat et al. [39, 40] and Rudraswamy et al. [41].

Even though, considerable progress has been made on three-dimensional flows of Jeffrey fluid over a linearly stretching surface in the presence of nonlinear thermal radiation, viscous dissipation, Joule heating, thermophoresis and Brownian motion effects. The governing systems of partial differential equations have been transformed to set of coupled ordinary differential equations by using suitable similarity transformations. The reduced equations are solved numerically. The pertinent parameters of Jeffery nanofluid are discussed through graphs and compare it with the tabulated results and plotted graphs. The present results are compared with the existing limiting solutions, showing good agreement with each other.

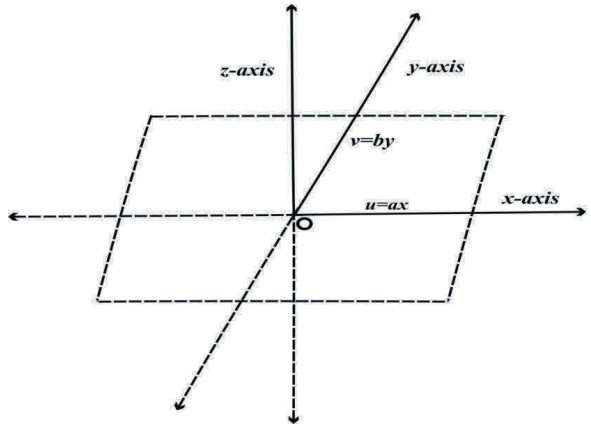

Fig. 1: Physical Flow.

2 Mathematical formulation

Consider a steady three-dimensional flow of an incompressible Jeffery fluid with suspended nanoparticles induced by bidirectional stretching surface at z = 0. The sheet is aligned with the xy-plane (z = 0) and the flow takes place in the domain $z > 0$. Let $u = U_w(x) = ax$ and $v = V_w(y) = by$ be the velocities of the stretching sheet along x and y directions respectively. A uniform magnetic field of strength B is applied in the z-direction. Heat and mass transfer characteristics are taken into account in the presence of nonlinear thermal radiation, Thermal-diffusion, Diffusion-thermo, Brownian motion and Thermophoresis effects. The thermophysical properties of the fluid are taken to be constant. The geometrical configuration of the present flow is shown in Fig. 1.

The governing boundary layer equations of momentum, energy and concentration equations for three-dimensional flow of Jeffry nanofluid can be written as,

$$\frac{\partial u}{\partial x}+\frac{\partial v}{\partial y}+\frac{\partial w}{\partial z}=0, \tag{1}$$

$$u\frac{\partial u}{\partial x}+v\frac{\partial u}{\partial y}+w\frac{\partial u}{\partial z}= \frac{\nu}{1+\lambda}\left(\frac{\partial^2 u}{\partial z^2}+\lambda_1\left(\begin{array}{l}\frac{\partial u}{\partial z}\frac{\partial^2 u}{\partial x\partial z}+\frac{\partial v}{\partial z}\frac{\partial^2 u}{\partial y\partial z}+\frac{\partial w}{\partial z}\frac{\partial^2 u}{\partial z^2}\\ +u\frac{\partial^3 u}{\partial x\partial z^2}+v\frac{\partial^3 u}{\partial y\partial z^2}+w\frac{\partial^3 u}{\partial z^3}\end{array}\right)\right)-\frac{\sigma B^2}{\rho}u, \tag{2}$$

$$u\frac{\partial v}{\partial x}+v\frac{\partial v}{\partial y}+w\frac{\partial v}{\partial z}= \frac{\nu}{1+\lambda}\left(\frac{\partial^2 v}{\partial z^2}+\lambda_1\left(\begin{array}{l}\frac{\partial u}{\partial z}\frac{\partial^2 v}{\partial x\partial z}+\frac{\partial v}{\partial z}\frac{\partial^2 v}{\partial y\partial z}+\frac{\partial w}{\partial z}\frac{\partial^2 v}{\partial z^2}\\ +u\frac{\partial^3 v}{\partial x\partial z^2}+v\frac{\partial^3 v}{\partial y\partial z^2}+w\frac{\partial^3 v}{\partial z^3}\end{array}\right)\right)-\frac{\sigma B^2}{\rho}v \tag{3}$$

$$\begin{aligned}u\frac{\partial T}{\partial x}+v\frac{\partial T}{\partial y}+w\frac{\partial T}{\partial z}&=\alpha\frac{\partial^2 T}{\partial z^2}\\ &+\tau\left[\begin{array}{l}D_B\frac{\partial T}{\partial z}\frac{\partial C}{\partial z}\\ +\frac{D_T}{T_\infty}\left(\frac{\partial T}{\partial z}\right)^2\end{array}\right]+\frac{2\mu}{\rho c_p}\left[\begin{array}{l}\left(\frac{\partial u}{\partial z}\right)^2\\ +\left(\frac{\partial v}{\partial z}\right)^2\end{array}\right]\\ &+\frac{\mu}{\rho c_p}\left[\begin{array}{l}\left(\frac{\partial^2 u}{\partial z^2}\right)^2+\\ \left(\frac{\partial^2 v}{\partial z^2}\right)^2\end{array}\right]+\frac{\sigma B^2}{\rho c_p}\left(u^2+v^2\right)\\ &-\frac{1}{(\rho c)_f}\frac{\partial q_r}{\partial z}+\frac{Dk_T}{c_s c_p}\frac{\partial^2 C}{\partial z^2}\end{aligned} \tag{4}$$

$$u\frac{\partial C}{\partial x}+v\frac{\partial C}{\partial y}+w\frac{\partial c}{\partial z}=D_B\frac{\partial^2 C}{\partial z^2}+\left(\frac{D_T}{T_\infty}+\frac{Dk_T}{T_m}\right)\frac{\partial^2 T}{\partial z^2} \tag{5}$$

The boundary conditions for the present flow analysis are,

$$\begin{aligned}&u=U_w(x)=ax,\ v=V_w(y)=by,\ w=0,\\ &T=T_w,\ C=C_w \text{ at } z=0,\end{aligned} \tag{6}$$

$$u\to 0,\ v\to 0,\ T\to T_\infty,\ C\to C_\infty \text{ as } z\to\infty, \tag{7}$$

where $\nu=\frac{\mu}{\rho}$ is the kinematic viscosity of the fluid, μ is the coefficient of fluid viscosity, ρ is the fluid density, λ_1 is the

relaxation time, B is the magnetic field, σ is the electrical conductivity of the fluid, T is the fluid temperature, $\alpha=\frac{k}{(\rho c)_f}$ is the thermal diffusivity of the fluid, k is the thermal conductivity. $\tau=\frac{(\rho c)_p}{(\rho c)_f}$ is the ratio of effective heat capacity of the nanoparticle material to heat capacity of the fluid, λ is the ratio of relaxation and retardation times, q_r is the radiative heat flux, D_B is the Brownian diffusion coefficient, D_T is the thermophoretic diffusion coefficient, c_s is the concentration susceptibility, k_T is the thermal diffusion ratio, T_m is the main fluid temperature, c_p is the specific heat at constant pressure, T_w and T_∞ are the temperatures of the surface and far away from the surface. C is the concentration and C_∞ are the concentration far away from the surface. The subscript w denotes the wall condition.

Using the Rosseland approximation for radiation, radiation heat flux q_r is simplified as,

$$q_r = -\frac{16\sigma^*}{3k^*}T^3\frac{dT}{dz}, \tag{8}$$

where σ^* and k^* are the Stefan–Boltzmann constant and the mean absorption coefficient respectively.

In view to equation (8), equation (4) reduces to

$$u\frac{\partial T}{\partial x}+v\frac{\partial T}{\partial y}+w\frac{\partial T}{\partial z}=\frac{\partial}{\partial z}\left[\left(\alpha+\frac{16\sigma^*T^3}{3k^*(\rho c)_f}\right)\frac{dT}{dz}\right]+\tau\left[\begin{array}{l}D_B\frac{\partial T}{\partial z}\frac{\partial C}{\partial z}\\+\frac{D_T}{T_\infty}\left(\frac{\partial T}{\partial z}\right)^2\end{array}\right]+\frac{2\mu}{\rho c_p}\left[\begin{array}{l}\left(\frac{\partial u}{\partial z}\right)^2\\+\left(\frac{\partial v}{\partial z}\right)^2\end{array}\right]+\frac{\mu}{\rho c_p}\left[\begin{array}{l}\left(\frac{\partial^2 u}{\partial z^2}\right)^2+\\\left(\frac{\partial^2 v}{\partial z^2}\right)^2\end{array}\right]+\frac{\sigma B^2}{\rho c_p}\left(u^2+v^2\right)+\frac{Dk_T}{c_s c_p}\frac{\partial^2 C}{\partial z^2} \tag{9}$$

The momentum, energy and concentration equations can be transformed into the corresponding ordinary differential equations by the following similarity variables,

$$u=axf'(\eta)\quad v=ayg'(\eta),\quad w=-\sqrt{av}\left(f(\eta)+g(\eta)\right),$$

$$\theta(\eta)=\frac{T-T_\infty}{T_W-T_\infty},\quad \phi(\eta)=\frac{C-C_\infty}{C_W-C_\infty},\quad \eta=\sqrt{\frac{a}{v}}, \tag{10}$$

where $T=T_\infty\left(1+(\theta_w-1)\,\theta(\eta)\right)$, $\theta_w=\frac{T_w}{T_\infty}$, $\theta_w>1$ being the temperature ratio parameter.

Then, we can see that equation (1) is automatically satisfied, and equations (2)–(7) are reduced as follows:

$$f'''+(1+\lambda)(f+g)f''-f'^2+\beta\left(f''^2-(f+g)f''''-g'f''\right)-(1+\lambda)Mf'=0 \tag{11}$$

$$g'''+(1+\lambda)(f+g)f''-f'^2+\beta\left(g''^2-(f+g)g''''-f'g''\right)-(1+\lambda)Mg'=0 \tag{12}$$

$$\frac{1}{Pr}\left(\left(1+R\left(1+(\theta_w-1)\,\theta\right)^3\right)\theta'\right)'+(f+g)\,\theta'+2\,\mathrm{Pr}\left(Ec_x f''^2+Ec_y g''^2\right)s-\mathrm{Pr}\left(Ec_x f'''^2+Ec_y g'''^2\right)+\mathrm{Pr}\,M\left(Ec_x f'^2+Ec_y g'^2\right)+N_b\theta'\varphi'+N_t\theta'^2+Df\phi''=0, \tag{13}$$

$$\phi''+LePr\,(f+g)\,\phi'+Sr\theta''+\left(\frac{N_t}{N_b}\right)\theta''=0. \tag{14}$$

The boundary conditions; will becomes:

$$f=0, g=0,\quad f'=1, g'=c\theta=1, \phi=1 \text{ at } \eta=0,$$

$$f'\to 0, g'\to 0,\quad \theta\to 0, \phi\to 0 \text{ as } \eta\to\infty, \tag{15}$$

where $\beta=\lambda_1 a$ is the Deborah number, $M=\frac{\sigma B^2}{\rho a}$ is the magnetic parameter, $c=\frac{b}{a}$ is the ratio of stretching rates, $Pr=\frac{v}{\alpha}$ is the Prandtl number, $R=\frac{16\sigma^* T_\infty^3}{3kk^*}$ is the radiation parameter, $N_b=\frac{\tau D_B(C_w-C_\infty)}{v}$ is the Brownian motion parameter, $N_t=\frac{\tau D_T(T_w-T_\infty)}{vT_\infty}$ is the Thermophoresis parameter, $Ec_x=\frac{U_w^2}{c_p(T_w-T_\infty)}$ and $Ec_y=\frac{V_w^2}{c_p(T_w-T_\infty)}$ is the Eckert number along x and y direction, $Sr=\frac{Dk_T(T_w-T_\infty)}{T_m v(C_w-C_\infty)}$ is the Soret number, $Df=\frac{Dk_T(C_w-C_\infty)}{c_s c_p v(T_w-T_\infty)}$ is the Dufour number, $Le=\frac{\alpha}{D_B}$ is the Lewis number and prime stands for order of derivatives with respect to η.

The local Nusselt number Nu_x and local number Sherwood Sh_x are defined as,

$$Nu_x=\frac{U_w q_w}{ka\,(T_w-T_\infty)},\quad Sh_x=\frac{V_w q_m}{D_b a(C_w-C_\infty)},$$

where q_w and q_m are the heat flux and mass flux respectively, which are given by;

$$q_w=\left(-k\frac{\partial T}{\partial z}+(q_r)_w\right)_{z=0},\quad q_m=-D_m\left(\frac{\partial c}{\partial z}\right)_{y=0}.$$

The local Nusselt number and Sherwood number is given by,

$$\frac{Nu_x}{(Re_x)^{\frac{1}{2}}}=-\left(1+Rd\theta_w^3\right)\theta'(0)\quad \frac{Sh_x}{(Re_x)^{\frac{1}{2}}}=-\phi(0),$$

where $Re_x=\frac{U_w^2(x)}{av}$ is the local Reynolds number.

3 Numerical Method

Equations (11) to (14) together with the boundary condition (15) from highly non-linear ordinary differential equations. In order to solve this nonlinear boundary value problem numerically by using Runge-Kutta-Fehlberg fourth-fifth order method along with shooting technique. In accordance with the boundary layer analysis, the boundary

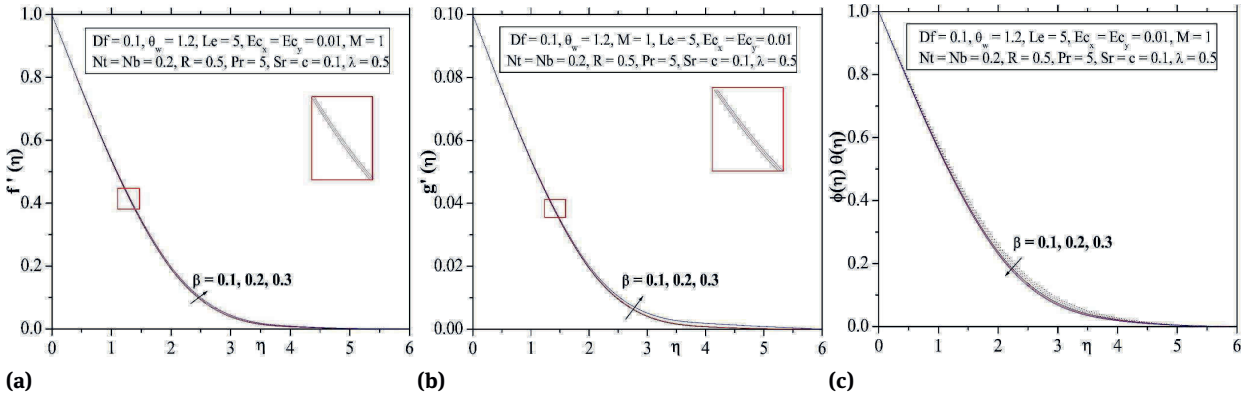

Fig. 2: Influence of β on velocity profiles of both (a) f' and (b) g', respectively. (c) Influence of λ on both $\theta(\eta)$ and (η) profiles.

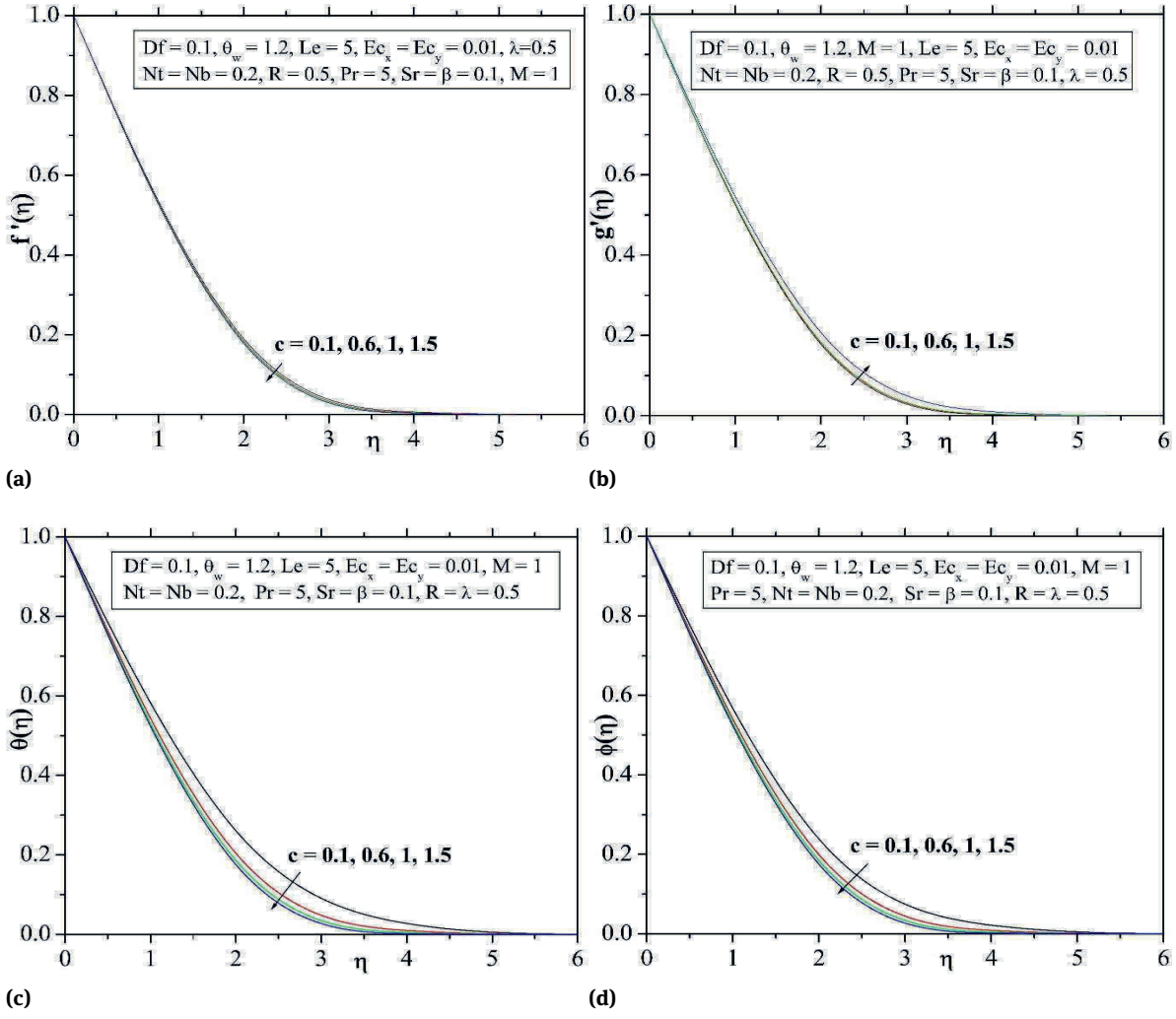

Fig. 3: Influence of c on velocity profiles of both (a) $f'(\eta)$ and (b) $g'(\eta)$, respectively. Influence of c on (c) $\theta(\eta)$ and $(d)\phi(\eta)$, respectively.

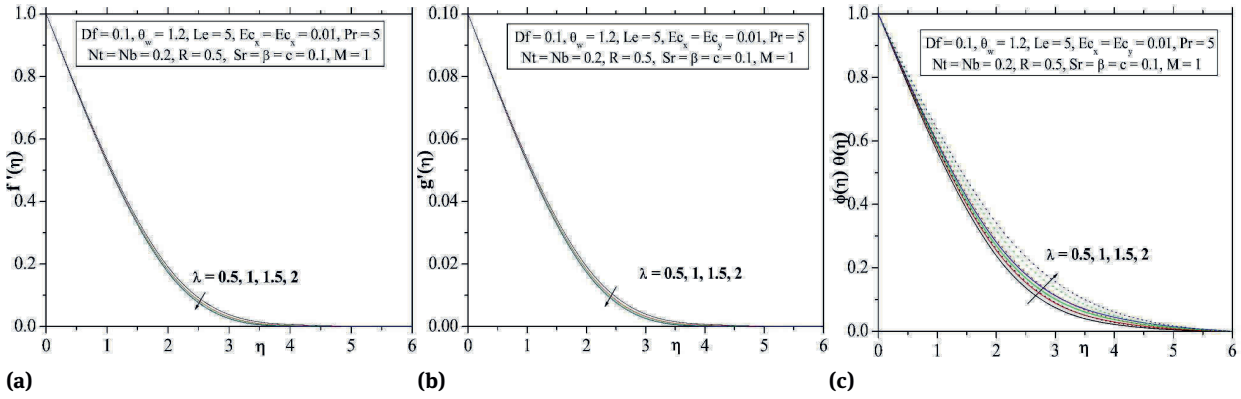

Fig. 4: Influence of λ on velocity profiles of both (a) $f'(\eta)$ and (b) $g'(\eta)$, respectively. (c) Influence of λ on both $\theta(\eta)$ and (η) profiles.

condition (15) at $\eta = \infty$ were replaced by $\eta = 6$. Table 1 shows the comparison of the present result with the previous results of Wang [32] and Hayat et al. [39] for various values of c. It shows good agreement with each other.

4 Result and Discussion

Numerical solutions for the current flow problem are obtained and tabulated for varying dimensional parameters over different fields. Observations over these data with plotted graphs are discussed below.

The dimensionless velocity, temperature and concentration profiles for different values of Deborah number (β) are sketched in Figures 2(a), 2(b) and 2(c), respectively. It is noticed that β responds positively over velocity profiles and negatively over for both temperature and concentration profiles. This is due to the fact that, β is directly proportional to the retardation time. Thus, the effect of Deborah number gives rise to higher retardation time and the higher retardation time increases the fluid flow due to which an enhancement is observed in the velocity profile.

Figure 3(a) and 3(b) depicts the velocity profiles of $f'(\eta)$ and $g'(\eta)$ for different values of stretching parameter (c). The velocity $f'(\eta)$ and the thickness of associated boundary layer decrease when the ratio parameter increases while Figure 3(b) exhibits the opposite behavior for $g'(\eta)$. Figure 3(c) and 3(d) demonstrate the effect of stretching ratio on both temperature profile and nanoparticle fraction respectively. It is observed that both the profiles downturn by the increase of stretching parameter. Figures 4(a) and 4(b) illustrate the influences of the ratio of relaxation to retardation times (λ) on the velocities profiles. From this figure we observed that the velocities $f'(\eta)$ and

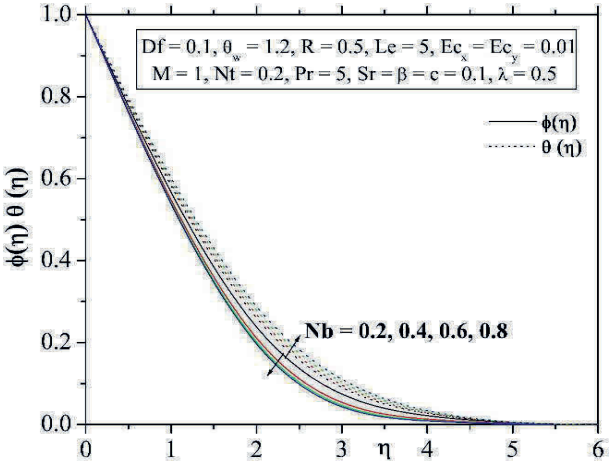

Fig. 5: Influence of Nb on both $\theta(\eta)$ and (η) profiles.

$g'(\eta)$ are decreasing functions of λ. Figure 4(c) represent the effect of λ on both temperature and concentration profile. Both temperature and concentration profile increases by increasing value of λ as well as corresponding boundary layer thickness also increases.

Figure 5 portraits the effects of Brownian motion parameter (Nb) on temperature and concentration profile. The Brownian motion parameter increases random motion of the fluid particles and boundary layer thickness also increases which results in more heat to produce. Hence temperature profile increases and concentration profile decreases.

Effect of a magnetic parameter (M) on the velocity profiles $f'(\eta)$ and $g'(\eta)$ illustrated in Figure 6(a) and 6(b). Here $M = 0$ corresponds to the hydrodynamic flow and $M >$ is for hydromagnetic flow. From these figures, it is observed that with the increase in the magnetic parameter, i.e. ratio of electromagnetic force to the viscous force, the velocity field decreases. This is due to the fact that, the Lorentz

Table 1: Comparison of different values of c with Wang [30] and Hayat et al. [37].

	Wang [30]		Hayatet et al. [37]		Present result	
c	$-f''(0)$	$-g''(0)$	$-f''(0)$	$-g''(0)$	$-f''(0)$	$-g''(0)$
0	1	0	1	0	1	0
0.25	1.0488	0.1945	1.048 810	0.194 57	1.04881	0.19457
0.5	1.0930	0.4652	1.093 095	0.465 205	109309	0.46522
0.75	1.1344	0.7946	1.134 500	0.794 620	1.13450	0.79462
1	1.1737	1.1737	1.173 721	1.173 721	1.17372	1.17372

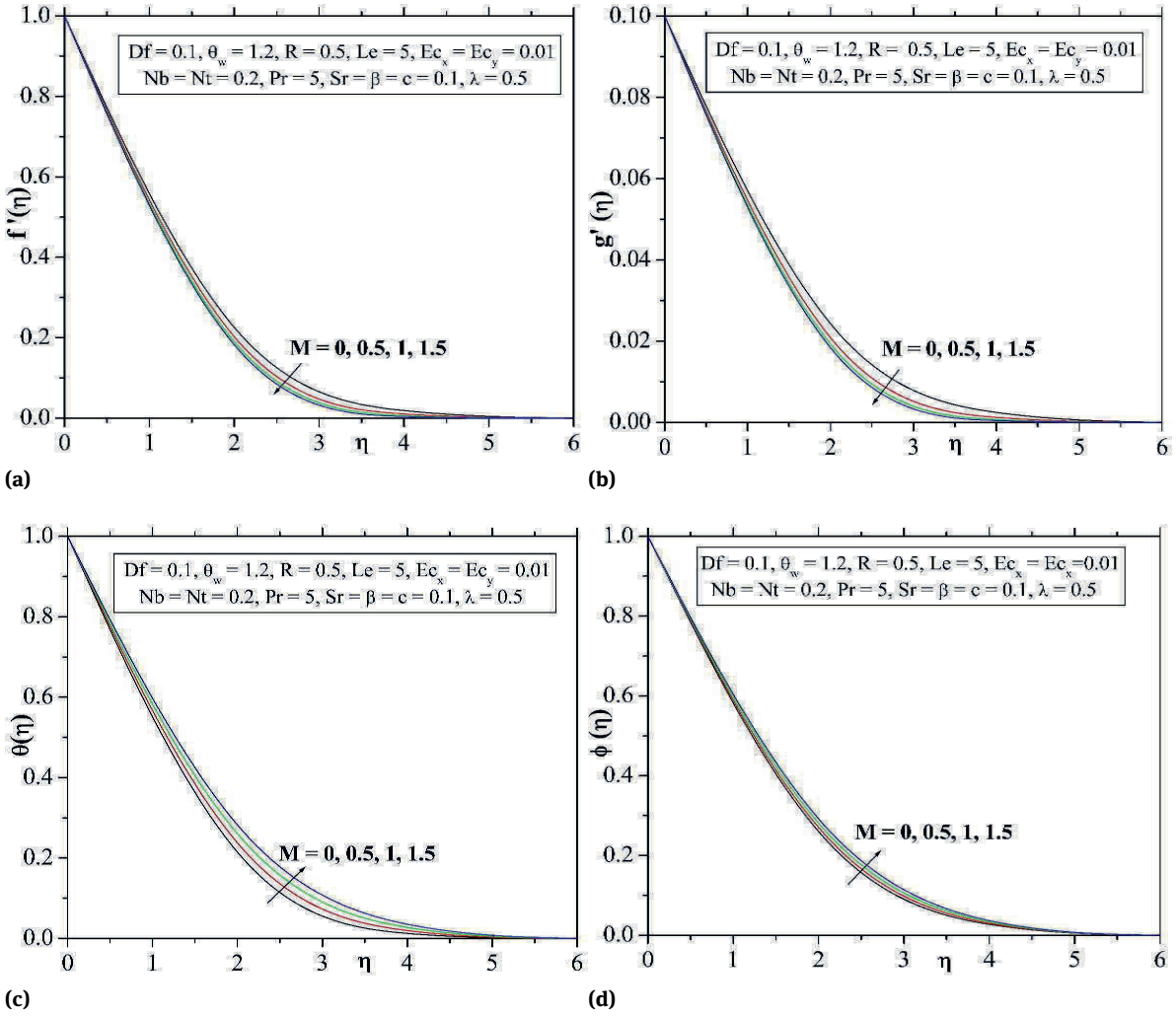

Fig. 6: Influence of M on velocity profiles of both (a) $f'(\eta)$ and (b) $g'(\eta)$, respectively. Influence of c on (c) $\theta(\eta)$ and $(d)\phi(\eta)$, respectively. Influence of M on (c) $\theta(\eta)$ and (d) $\phi(\eta)$, respectively.

force appeared in hydromagnetic flow due to presence of magnetic parameter. We know that, the Lorentz force is stronger corresponding to larger magnetic parameter due to which enhances the temperature and thermal boundary layer. As the value of M increases, the retarding force increases and consequently the velocity decreases. But in the case of temperature and concentration profiles it exhibit opposite behavior of velocity profiles. shown in Figure 6(c) and 6(d).

The effects of the thermophoresis parameter (Nt) on $\theta(\eta)$ and $\phi(\eta)$ can be seen in Figure 7(a) and 7(b). An increase in the values of thermophoresis parameter increases both $\theta(\eta)$ and $\phi(\eta)$ profiles. Thermal boundary layer thickness is higher for larger values of thermophore-

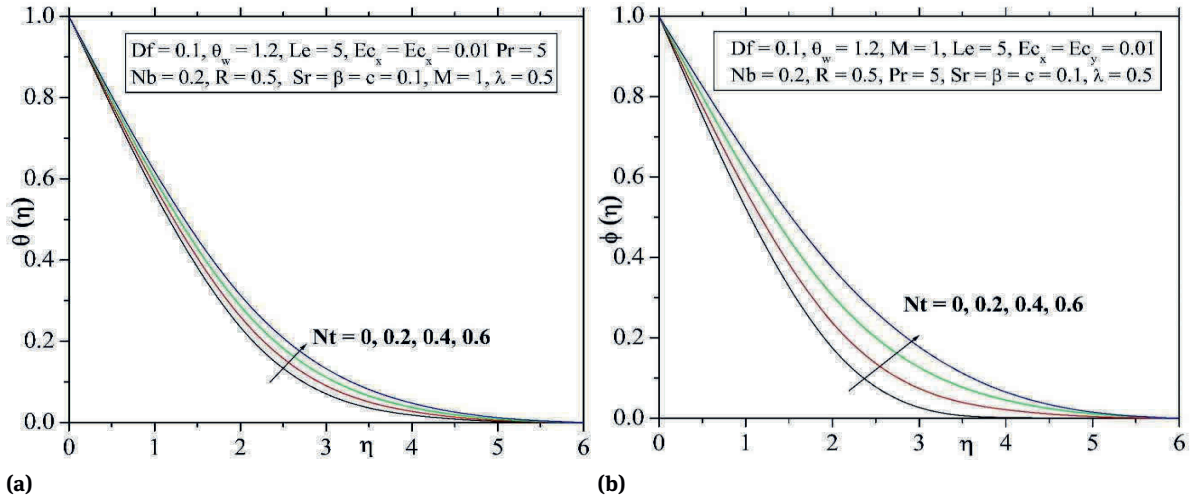

Fig. 7: Influence of Nt on (a) $\theta(\eta)$ and (b) $\phi(\eta)$, respectively.

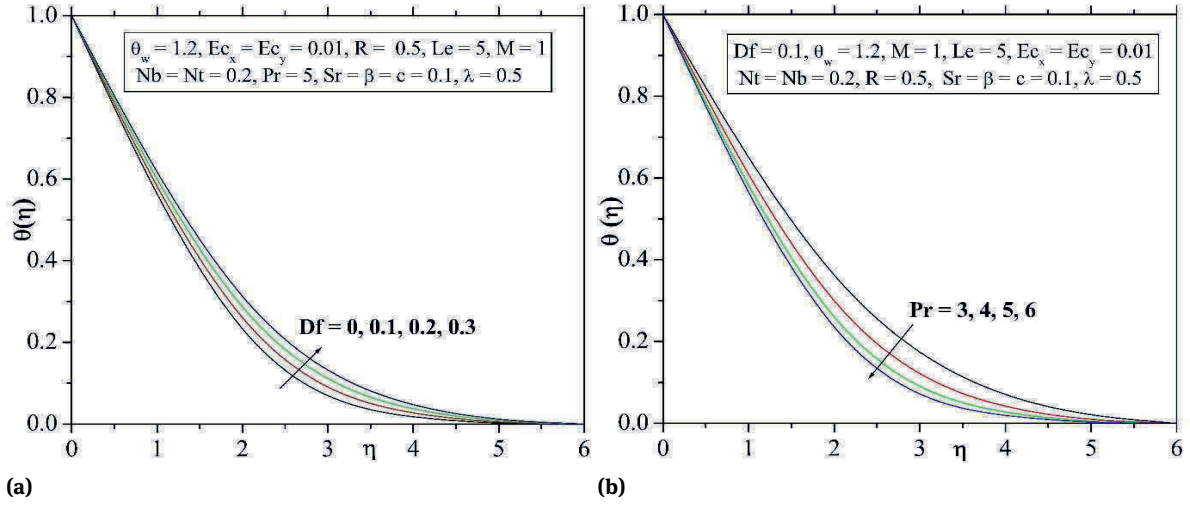

Fig. 8: Influence of (a) Df and (b) Pr on temperature profile.

sis parameter. It is a mechanism in which small particles are pulled away from the hot surface to a cold one. As a result, it raises the temperature and concentration of the fluid.

Figure 8(a) shows the effect of Dufour parameter (Df) for temperature profile. An uplifting the values of Dufour parameter increases the temperature profile and corresponding boundary layer thickness. The effects of the Prandtl number (Pr) on $\theta(\eta)$ can be seen in Figure 8(b). Since Pr is the ratio of the viscous diffusion rate to the thermal diffusion rate, higher value of Prandtl number causes to reduce the thermal diffusivity. Consequently, for increasing values of Pr temperature profile decreases.

Figure 9(a) and 9(b) represents the effect of temperature ratio parameter and radiation for temperature profile respectively. Temperature profile and thermal boundary layer thickness are enhanced by increasing the values of radiation parameter (R) and temperature ratio (θ_w). This is due to the fact that larger values of radiation parameter provide more heat to working fluid that shows an enhancement in the temperature field. The thermal boundary layer thickness also shows a positive response for an increasing R. Figure 10(a) and 10(b) are plotted to show the temperature distributions for contrasting values of Eckert numbers. It is observed that both thermal boundary layer thickness increase for increasing value of Eckert numbers. This is due to the presence of viscous dissipation in the en-

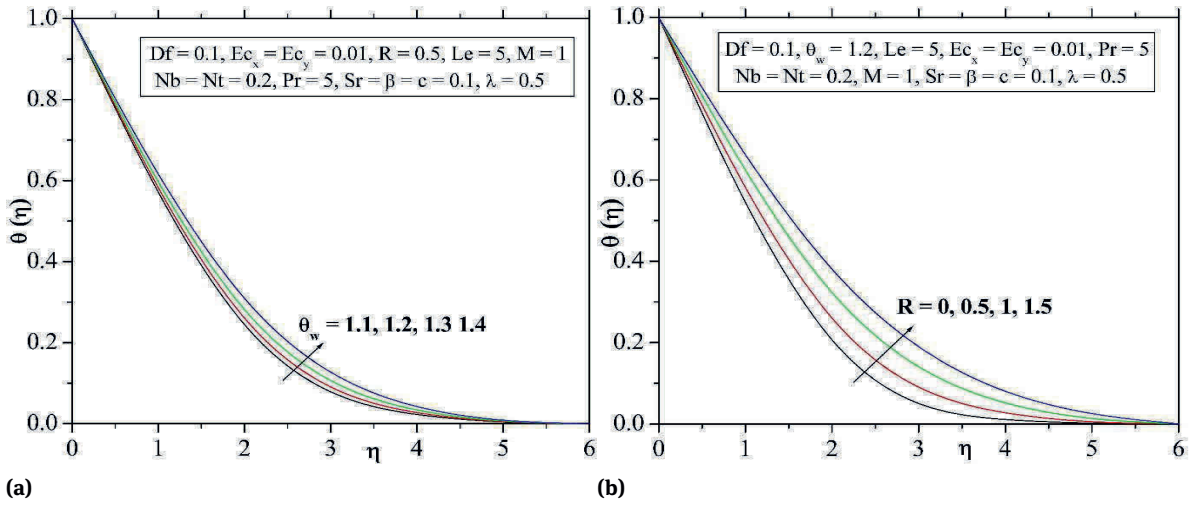

Fig. 9: Influence of (a) θ_w and (b) R on temperature profile.

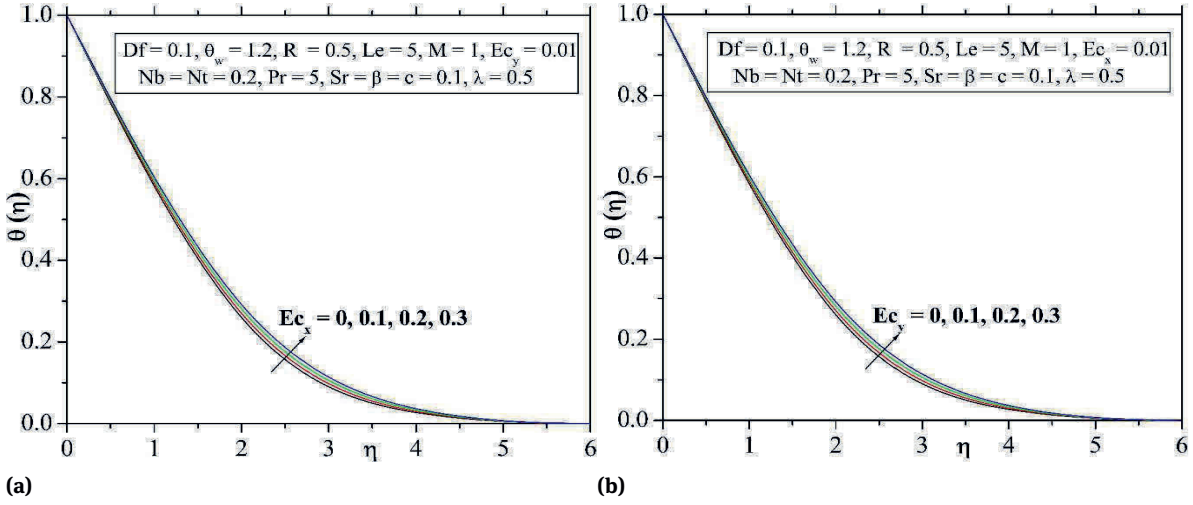

Fig. 10: Influence of Eckert numbers on temperature profile.

ergy equation which acts as an internal heat source that increases the thermal energy and thus heat the regime.

Figure 11(a) illustrates the influences of the Soret (Sr) parameter on the concentration profile. It is observed that the nanoparticles concentration and associated thermal boundary layer thickness are enhanced by increasing Soret parameter. The impact of Lewis number (Le) on concentration profile is shown in Figure 11(b). It is evident that higher values of Lewis number cause a reduction in concentration distribution. Lewis number depends on the Brownian diffusion coefficient. Larger Lewis number leads to the lower Brownian diffusion coefficient, which shows a weaker nanoparticle concentration.

Influence of Le and Ec_x on Nusselt number is sketched in Figure 12(a). It is analyzed that Nusselt number increases for higher values ofLe and Ec_x, the same behavior as shown in Figure 12(b) by increasing values of Nb an Nt. Figur 12 (c) illustrate the influences of R with the various values of Pron Nusselt number. It is clear Nusselt number increases by increasing the values of R and Pr. Characteristics of Sr and Le on Sherwood number is displayed in Figure 13(a). Sherwood number increase by an uplifting the values of Sr and Le. But, the Sherwood number decrease by increasing the values of λ and Sr asshown in Figure 13(b).

Table 2 presents the numerical values of Nusselt number and Sherwood number for various physical parameter. It is observed that Nusselt number increase and Sherwood number decreases with increasing Df, θ_w, Ec_x, Ec_y and

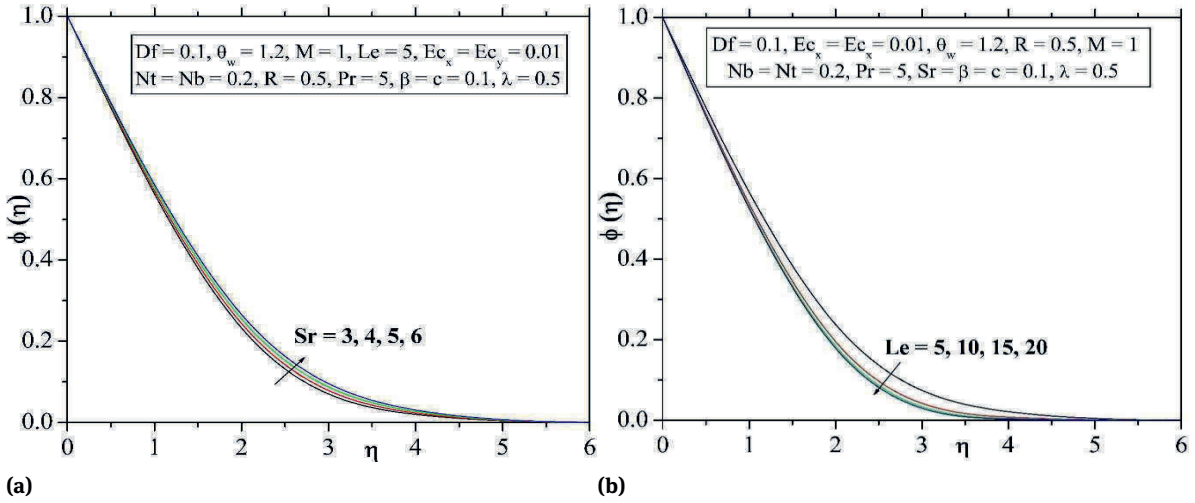

Fig. 11: Influence of Sr and Le on concentration profile.

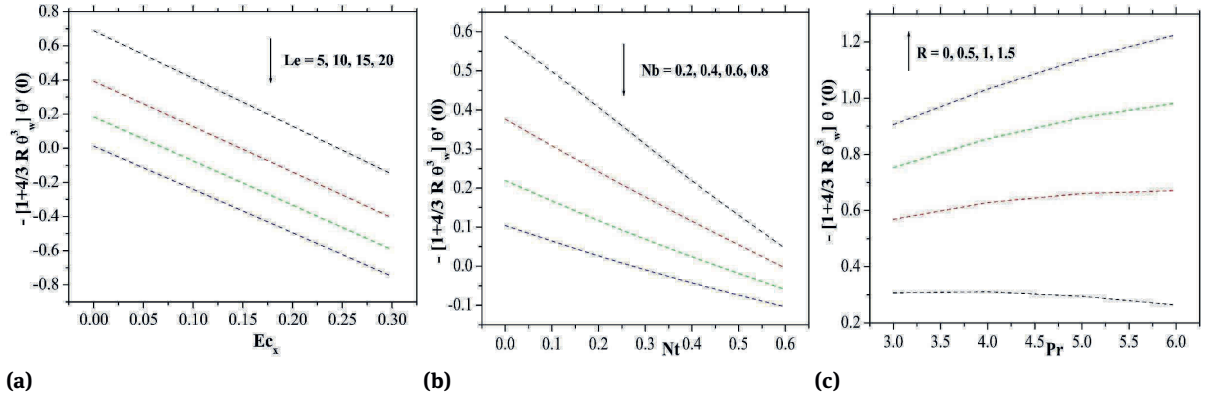

Fig. 12: Influence of Le and Nb with the various values of Ec_x and Nt on Nusselt number. (c) represents the influence of R with the various values of Pr on Nusselt number.

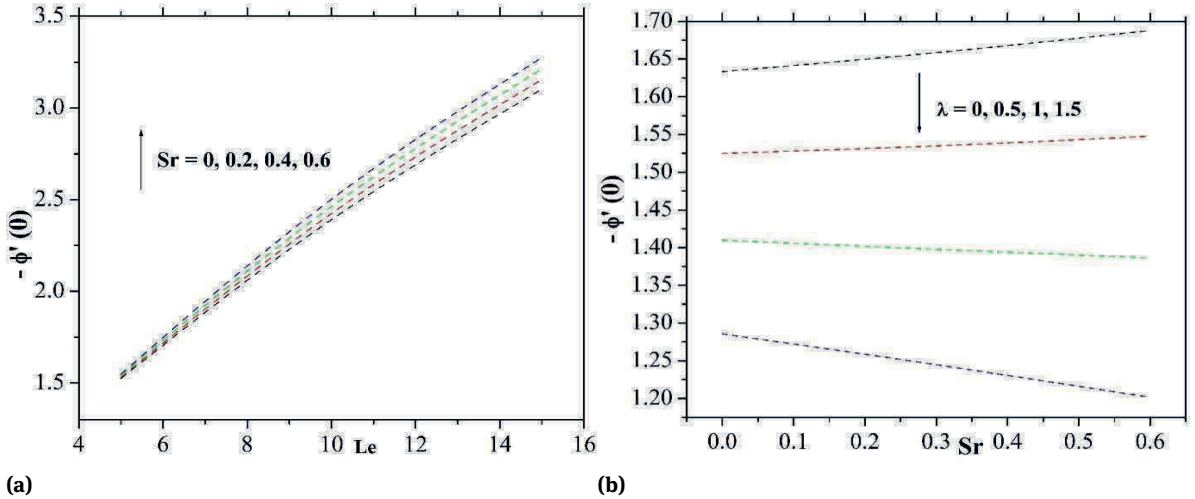

Fig. 13: Influence of Sr and λ with the various values of Le and Sr on Sherwood number.

Table 2: Values of Sherwood number $-Re_x^{-\frac{1}{2}} Sh_x$ and Nusselt number $-Re_x^{-\frac{1}{2}} Nu_x$ for the different values of the parameters.

D_f	θ_w	Ec_x	Ec_y	Le	M	Nb	R	Nt	Pr	Sr	β	c	λ	$-Re_x^{-\frac{1}{2}} Nu_x$	$-Re_x^{-\frac{1}{2}} Sh_x$
0														1.30925	0.99564
0.1														1.42346	0.66029
0.2														1.58296	0.21630
	1.1													1.42014	0.71740
	1.2													1.42346	0.66029
	1.3													1.42951	0.60079
		0												1.41191	0.68807
		0.1												1.52786	0.40956
		0.2												1.64474	0.12946
			0											1.40734	0.62129
			0.5											1.44346	0.60029
			1											1.43960	0.59925
				5										1.42346	0.61029
				10										2.35689	0.36590
				15										3.04562	0.15753
					0									1.46468	0.77024
					0.5									1.48724	0.70752
					1									1.52346	0.66029
						0.2								1.42346	0.66029
						0.4								1.50043	0.45465
						0.6								1.52173	0.30853
							0							1.48285	0.63433
							0.5							1.42346	0.62029
							1							1.41719	0.60634
								0.2						1.42346	0.66029
								0.4						1.44157	0.50854
								0.6						1.57808	0.33907
									3					1.42015	0.56827
									4					1.41733	0.62819
									5					1.40346	0.66029
										0				1.42346	0.66029
										0.2				1.44157	0.50854
										0.4				1.57808	0.33907
											0.1			1.41015	0.56827
											0.2			1.42733	0.62819
											0.3			1.46129	0.68422
												0.1		1.42346	0.66029
												0.6		1.78223	0.85322
												1		2.02548	0.98151
													0.5	1.42346	0.66029
													1	1.34846	0.61971
													1.5	1.28422	0.59324

Le. But an increase the values of Pr, β and c increases the Nusselt and Sherwood number.

5 Conclusion

In the present analysis, effect of viscous dissipation and Joule heating in three-dimensional flow of Jeffrey nano fluid in the presence of nonlinear thermal radiation is performed numerically. Effects of various parameters are studied graphically. The main points of the present simulations are listed as follows:

- Magnetic field and ratio of relaxation time to retardation parameter reduce the velocity profiles in both the directions.
- The impacts of the Brownian motion parameter on the temperature and concentration fields are quite opposite.

- The concentration profile and corresponding boundary layer thickness increases with an increasing values of Sr
- The velocity profile $f^{'}(\eta)$ decrease with the increase of the parameter c but velocity profile $g^{'}(\eta)$ is quite opposite when the parameters c increase.
- The rate of heat transfer increases with the increases in parameters Rd, Df and θ_w while decreases when Pr increase.
- A raise in the value of Deborah number enhances the momentum boundary layer thickness in both x– and y–directions and depreciates the heat transfer rate. Thus coolants with small Deborah number are best suitable for cooling heated sheets.
- We also noticed that the nanoparticle concentration and its associated boundary layer thickness are decreased when we gradually increase the values of Lewis number.
- The combined effects of Joule heating and viscous dissipation increase the temperature profile and thermal boundary layer thickness.
- Nonlinear thermal radiation should be kept minimum to use it as a coolant factor.

References

[1] H.I. Andersson, K.H. Bech and B.S. Dandapat, "Magnetohydrodynamic flow of a power-law fluid over a stretching sheet", *Int. J. Non-Linear Mech.,* Vol. 27 no. 6, pp. 929–936, 1992.

[2] Shi-Jun Liao, "On the analytic solution of magnetohydrodynamic flows of non-Newtonian fluids over a stretching sheet", *J. of Fluid Mech.,* Vol. 488,pp. 189–212, 2003.

[3] M. Subhas Abeland N. Mahesha, "Heat transfer in MHD viscoelastic fluid flow over a stretching sheet with variable thermal conductivity, non-uniform heat source and radiation", *Appl. Math. Model.,* Vol.32, no.10, pp. 1965–1983, 2008.

[4] R. Nazar, N. Amin, D. Filip, and I. Pop, "Stagnation point flow of a micropolar fluid towards a stretching sheet,"*Int. J. Non-Linear Mech.,* Vol. 39, no. 7, pp. 1227–1235, 2004.

[5] R.K. Bhatnagar, G. Gupta and K.R. Rajagopal, "Flow of an Oldroyd-B fluid due to a stretching sheet in the presence of a free stream velocity", *Int. J. Non-Linear Mech.,* Vol. 30, no. 3, pp. 391–405, 1995.

[6] R. Cortell, "A note on magnetohydrodynamic flow of a power-law fluid over a stretching sheet", *Appl. Math. Comp.,* Vol. 168, no. 1, pp. 557–566, 2005.

[7] R.C. Bataller, "Viscoelastic fluid flow and heat transfer over a stretching sheet under the effects of a non-uniform heat source, viscous dissipation and thermal radiation", *Int. J. Heat Mass Trans.,* Vol. 50, no. 15–16, pp. 3152–3162, 2007.

[8] I.L. Animasaun, C.S.K. Raju and N. Sandeep, "Unequal diffusivities case of homogeneous–heterogeneous reactions within viscoelastic fluid flow in the presence of induced magnetic-field and nonlinear thermal radiation", *Alexandria Engg. J.,* Vol. 55, no. 2, pp. 1595–1606, 2016.

[9] P.G. Siddheshwar and U.S. Mahabaleshwar, "Effects of radiation and heat source on MHD flow of a viscoelastic liquid and heat transfer over a stretching sheet", *Int. J. Non-Linear Mech.,* Vol. 40, no. 6, pp. 807–820, 2005.

[10] V. Aliakbar, A.A. Pahlavan and K. Sadeghy, "The influence of thermal radiation on MHD flow of Maxwellian fluids above stretching sheets", *Comm. Nonlinear Sci. Numer. Simul.,*Vol. 14, no. 3, pp.779-794, 2009.

[11] Dulal Pal "Heat and mass transfer in stagnation-point flow towards a stretching surface in the presence of buoyancy force and thermal radiation", *Meccanica*, Vol. 44, pp. 145–158, 2009.

[12] M.A.A. Mahmoud, "Thermal radiation effects on MHD flow of a micropolar fluid over a stretching surface with variable thermal conductivity", *Physica A: Statistical Mech. Appli.*, Vol. 375, no. 2, pp. 401–410, 2007.

[13] M.N. Mahantesh, K. Vajravelu and M.S. Abel, "Heat transfer in MHD viscoelastic boundary layer flow over a stretching sheet with thermal radiation and non-uniform heat source/sink", *Comm. Nonlinear Sci. Numer. Simul.*, Vol. 16, no. 9, pp. 3578–3590, 2011.

[14] T.C. Chiam, "Magnetohydrodynamic Heat Transfer Over a Non-Isothermal Stretching Sheet", *Acta Mech.,* Vol. 122, pp. 169-179, 1997.

[15] R. Cortell, "Effects of viscous dissipation and work done by deformation on the MHD flow and heat transfer of a viscoelastic fluid over a stretching sheet", *Physics Letters A.,* Vol. 357, no. 4-5, pp. 298-305, 2006.

[16] A.A. Mohammadein and R.S.R. Gorla, "Heat transfer in a micropolar fluid over a stretching sheet with viscous dissipation and internal heat generation," *Int. J. Numer. Methods Heat Fluid Flow*, Vol. 11, no. 1, pp. 50–58, 2001.

[17] T. Hayat and A. Alsaedi, "Thermal radiation and Joule heating effects in MHD flow of an Oldroyd-B fluid with thermophoresis", *Arab J. Sci. Engg.,* Vol. 36, pp. 1113–1124, 2011.

[18] N.G. Kafoussias and E.W. Williams, " Thermal-diffusion and diffusion-thermo effects on mixed free-forced convective and mass transfer boundary layer flow with temperature dependent viscosity", *Int. J. Engg. Sci.,* Vol. 33, no. 9, pp. 1369–1384, 1995.

[19] D. Srinivasacharya and K. Kaladhar, "Mixed convection flow of couple stress fluid in a non-darcyporous medium with Soret and Dufour effects", *J. Appl. Sci. Engg.*, Vol. 15, pp. 415–422, 2012.

[20] T. Hayat, S.A. Shehzadand A. Alsaedi, "Soret and Dufour effects on MHD flow of Casson fluid", *Appl. Math. Mech. (English Edition),* Vol. 33, pp. 1301–1312, 2012.

[21] S. Nadeem, R. UlHaq, and N. S. Akbar "MHD three-dimensional boundary layer flow of Casson nanofluid past a linearly stretching sheet with convective boundary condition", *IEEE. Trans. on Nanotech*, Vol. 13, no. 1, pp. 109–115, 2014.

[22] C. Sulochana, S.S. Payad and N. Sandeep, "Non-uniform heat source or sink effect on the flow of 3D Casson fluid in the presence of Soret and thermal radiation", *Int. J. Engg. Research in Africa,* Vol. 20, pp. 112–129, 2015.

[23] N. Anbuchezhian, K. Srinivasan, K. Chandrasekaran and R. Kandasamy, "Thermophoresis and Brownian motion effects

on boundary layer flow of nanofluid in presence of thermal stratification due to solar energy", *Appl. Math. and Mech. (English Edition),* Vol. 33, pp. 765–780, 2012.

[24] S.U.S.Choi, "Enhancing thermal conductivity of fluid with nanoparticles, developments and applications of non-Newtonian flow", *ASME FED.*, Vol. 231, pp. 99–105, 1995.

[25] W.A. Khan and I. Pop "Boundary-layer flow of a nanofluid past a stretching sheet", *Int. J. Heat Mass Trans.,* Vol. 53, no. 11–12, pp. 2477–2483, 2010.

[26] M. Mustafa, T. Hayat, I. Pop, S. Asghar and S. Obaidat, "Stagnation-point flow of a nanofluid towards a stretching sheet", *Int. J. Heat Mass Trans.,* Vol. 54, no. 25–26, pp. 5588–5594, 2011.

[27] O.D. Makinde, W.A. Khan and Z.H. Khan, "Buoyancy effects on MHD stagnation point flow and heat transfer of a nanofluid past a convectively heated stretching/shrinking sheet", *Int. J. Heat Mass Trans.,* Vol. 62, pp. 526–533, 2013.

[28] N.G. Rudraswamy and B.J. Gireesha, "Influence of chemical reaction and thermal radiation on MHD boundary layer flow and heat transfer of a nanofluid over an exponentially stretching sheet", *JAMP*, Vol. 2, No.2, pages 9, 2014.

[29] T. Hussain, S.A. Shehzad, T. Hayat, A. Alsaedi, F. Al-Solamy, M. Ramzan, "Radiative Hydromagnetic Flow of Jeffrey Nanofluid by an Exponentially Stretching Sheet", PLoS ONE 9(8): e103719, (2014).

[30] N. Sandeep, B. Rushi Kumar and M.S. Jagadeesh Kumar , "A comparative study of convective heat and mass transfer in non-Newtonian nanofluid flow past a permeable stretching sheet", *J. Molec. Liq.*, Vol. 212, pp. 585–591, 2015

[31] B.J. Gireesha, A.J. Chamkha, N.G. Rudraswamy and M.R. Krishnamurthy, "MHD flow and heat transfer of a nanofluid embedded with dust particles over a stretching sheet," J. Nanofluids, Vol. 4, no. 1, pp. 66–372, 2015.

[32] C.Y. Wang, "The three-dimensional flow due to a stretching sheet", *Phys. Fluids*, Vol. 27, pp. 1915–1917, 1984.

[33] T. Hayat, M.Imtiaz, A. Alsaedi and M.A. Kutbi, "MHD three-dimensional flow of nanofluid with velocity slip and nonlinear thermal radiation", *JMMM,* Vol. 396, pp. 31–37, 2015.

[34] M. Ahmad. I. Ahmad and M. Sajid, "Magnetohydrodynamic time dependent three-dimensional flow of Maxwell fluid over a stretching surface through porous space with variable thermal conditions," *J. Braz. Soc. Mech. Sci. Eng.,* Vol. 38, pp. 1767–1778, 2016.

[35] K. Ruba and M. Mustafa, "Cattaneo-christov heat flux model for MHD three-dimensional flow of Maxwell fluid over a stretching sheet", *PLoS ONE,* Vol. 11, no. 4, e0153481, 2016.

[36] T.Hayat, T. Muhammad, B. Ahmad and S.A.Shehzad, "Impact of magnetic field in three-dimensional flow of Sisko nanofluid with convective condition, "*JMMM,* Vol. 413, pp. 1–8, 2016.

[37] M. Ramzan and M. Bilal, "Three-dimensional flow of an Elastico-viscous nanofluid with chemical reaction and magnetic field effects," *J. Molec. Liq.,* vol. 215, pp. 212–220, 2016.

[38] S.A. Shehzad, Z. Abdullah, A. Alsaedi, F.M. Abbasi and T. Hayat, "Thermally radiative three-dimensional flow of Jeffrey nanofluid with internal heat generation and magnetic field", *J. of Magn. and Mag. Mate.,* Vol. 397, pp. 108–114, 2016.

[39] T. Hayat, S.A. Shehzad, and A. Alsaedi, "Three-dimensional stretched flow of Jeffrey fluid with variable thermal conductivity and thermal radiation*", Appl. Math. Mech. -Engl. Ed.,* Vol. 34, no. 7, pp. 823–832, 2013.

[40] T. Hayat, M. Waqas, S.A. Shehzad and A. Alsaedi, "A model of solar radiation and Joule heating in magnetohydrodynamic (MHD) convective flow of thixotropic nanofluid", *J. Molec. Liq.*, Vol. 215, pp. 704–710, 2016.

[41] N.G. Rudraswamy, K.G. Kumar, B.J. Gireesha, R.S.R. Gorla, "Combined effect of joule heating and viscous dissipation on MHD three dimensional flow of a jeffrey nanofluid", *J. Nanofluids*, Vol. 6, no. 2, pp. 300–310, 2017.